Short-term Spectral Analysis and Synthesis improvements with oversampled inverse filter banks

Jérôme Gauthier[a,b] and Laurent Duval[a]

[a]Institut Français du Pétrole, IFP, Technology, Computer Science and Applied Mathematics, 1 et 4, avenue de Bois-Préau, 92852 Rueil-Malmaison Cedex, France

[b]Institut Gaspard Monge and UMR CNRS 8049, Université de Paris-Est Marne-La-Vallée, 77454 Marne-La-Vallée Cedex 2, France

ABSTRACT

The Short Term Fourier Transform (STFT) is a classical linear time-frequency (T-F) representation. Despites its relative simplicity, it has become a standard tool for the analysis of non-stationary signals. Since it provides a redundant representation, it raises some issues such as (i) "optimal" window choice for analysis, (ii) existence and determination of an inverse transformation, (iii) performance of analysis-modification-synthesis, or reconstruction of selected components of the time-frequency plane and (iv) redundancy controllability for low-cost applications, *e.g.* real-time computations. We address some of these issues, as well as the less often mentioned problem of transform symmetry in the inverse, through oversampled FBs and their optimized inverse(s) in a slightly more general setting than the discrete windowed Fourier transform.

Keywords: Time-frequency analysis, Oversampled Filter Bank, Short Term Fourier Transform, Inverse Filter optimization.

1. BACKGROUND AND PROPOSED WORK

Let $x(t)$ be a continuous time signal and $h(t)$ an analysis window, both with finite energy. The standard continuous time STFT with window $F_x(t, \nu; h)$ resorts to pre-windowing the signal x at a particular time t and computing the Fourier transform of the result:[1]

$$F_x(t, \nu; h) = \int_{-\infty}^{+\infty} x(u) h^*(u - t) e^{-\imath 2\pi\nu u} du \,.$$

The signal may be perfectly recovered from its STFT with a synthesis window $g(t)$, in general different from $h(t)$, with the formula:[1,2]

$$x(t) = \int_{-\infty}^{+\infty} \int_{-\infty}^{+\infty} F_x(u, \xi; h) g(t - u) e^{\imath 2\pi t u} du d\xi,$$

provided the windows satisfy the following equation:

$$\int_{-\infty}^{+\infty} g(t) h^*(t) dt = 1. \qquad (1)$$

Further author information, send correspondence to: {jerome.gauthier,laurent.duval}@ifp.fr

Provided that the window $h(t)$ has unit-energy, a typical window choice is $g(t) = h(t)$, but depending on the application, due to the relatively mild condition of Eq. (1), other carefully designed reciprocal synthesis windows may be chosen.[3] For practical applications, the STFT may be discretized regularly in the time-frequency plane and applied to a discrete signal $x(k)$. As long as the discrete window $h(k)$ does not vanish on its support, the signal may be recovered from its discrete STFT via weighted overlap-add procedures.[4,5] Such a simple Fourier-plus-window inversion may lead to artifacts after time-frequency cancellations. Kramer *et al.* improved such a localized time-frequency filtering by a least-square reconstruction leading to a pseudo-inverse formulation for the synthesis operator.[6] Additionally, the authors proposed an optimal design for the analysis windows. It should be noted that, in the discrete case, the standard conditions to be satisfied for a couple of admissible analysis-synthesis windows are far more stringent.[7] Thus, the choice and optimization of appropriate window pairs is *a priori* more complex. Additionally, standard STFT implementations with one-sample step in time are highly redundant. Early works address for instance the reconstruction of signals from irregularly STFT samples[8,9] using projection onto convex sets. Recently, the characterization and theoretical construction of oversampled FBs has generated a renewed interest.[10–13] The practical advantages in terms of design and robustness have promoted their use in applications such as in multiple description coding,[14] source separation,[15] channel equalization[16] or directional seismic image filtering.[17] The aim of this work is to address some of the aforementioned issues in the filter bank (FB) framework in the context of real-time T-F filtering of mixed real, one-dimensional signals, using recent results on the optimization of inverse oversampled FBs,[18] rooted on a pseudo-inverse initial solution. Since the STFT may be considered as an oversampled FB, we propose to locally filter signals of interest in the T-F domain with optimized analysis-synthesis oversampled FBs. We take advantage of the degrees of freedom in the FB design to reduce the computational complexity of the transform with respect to the STFT while preserving the noise robustness.

In Section 2, we first recall the polyphase notations used in this work before explaining how to invert an overlapping and oversampled FB. This inverse problem, being underdetermined due to the redundancy, we explain how to design, through an optimization process, a synthesis FB with good frequency selection. To apply the FB on real-valued signals and ensure a real-valued reconstruction, we study the Hermitian symmetry property of synthesis FB in Section 2.4. In Section 3, we provide examples of synthesis FB using the different construction methods proposed previously. We finally compare the reconstruction properties of optimized FB with the STFT, on real and simulated data.

2. FILTER BANK CONSTRUCTION

In this section we briefly review how to invert an oversampled and overlapping filter bank. We then see how to exploit the redundancy of the problem to choose a synthesis FB with good frequency selection. Finally we propose a method to ensure that the synthesis FB offers the Hermitian symmetry property, which is important for applications on real-valued signal.

2.1. Notations

We first recall the polyphase notations used throughout this work for the 1D M-band filter bank structure represented Figure 1. The sampled signal $(x(n))_{n\in\mathbb{Z}}$ is transformed using M filters with impulse responses: $(h_i)_{0\leq i<M}$, each one having finite length kN with $k \in \mathbb{N}^*$. A decimation by an integer N is then performed. From a lapped transform viewpoint,[19] there are therefore $k-1$ overlapping blocks of size N. The M outputs of

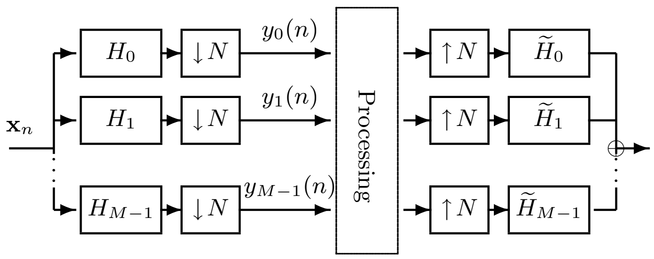

Figure 1. M/N oversampled M-channel filter banks.

the analysis FB are denoted by $(y_i(n))_{0\leq i<M}$. The overall redundancy of the transform is thus $M/N = k'$. In this work we focus on the oversampled case, *i.e.* $k' > 1$.

With these notations, the outputs of the analysis FB are expressed, for all $i \in \{0, \ldots, M-1\}$ and $n \in \mathbb{Z}$, as

$$\begin{aligned} y_i(n) &= \sum_p h_i(p)x(Nn-p) \\ &= \sum_\ell \sum_{j=0}^{N-1} h_i(N\ell+j)x(N(n-\ell)-j). \end{aligned} \tag{2}$$

Let $\boldsymbol{H}(\ell) = (h_i(N\ell+j))_{0\leq i<M, 0\leq j<N}$, $\ell \in \{0, \cdots, k-1\}$ be the k matrices obtained from the impulse responses of the filters. The polyphase vector signal from the input signal $x(n)$ is then defined as: $\forall n \in \mathbb{Z}$, $\mathbf{x}(n) = (x(Nn-j))_{0\leq j<N}$. Equation (2) can be rewritten in a more concise form:

$$\begin{aligned} \mathbf{y}(n) &= (y_0(n), \ldots, y_{M-1}(n))^\top \\ &= \sum_\ell \boldsymbol{H}(\ell)\mathbf{x}(n-\ell) = (\boldsymbol{H} * \mathbf{x})(n), \end{aligned}$$

or, equivalently, $\mathbf{y}[z] = \boldsymbol{H}[z]\mathbf{x}[z]$, where $\boldsymbol{H}[z] = \sum_{\ell=0}^{k-1} \boldsymbol{H}(\ell)z^{-\ell}$ is the $M \times N$ polyphase transfer matrix of the analysis filter bank and $\mathbf{x}[z]$ and $\mathbf{y}[z]$ are the z-transforms of $(\mathbf{x}(n))_{n\in\mathbb{Z}}$ and $(\mathbf{y}(n))_{n\in\mathbb{Z}}$, respectively. Similarly, we define the polyphase transfer matrix of the synthesis filter bank: $\widetilde{\boldsymbol{H}}[z] = \sum_\ell \widetilde{\boldsymbol{H}}(\ell)z^{-\ell}$ which is such that

$$\widetilde{\mathbf{x}}[z] = \widetilde{\boldsymbol{H}}[z]\mathbf{y}[z].$$

The polyphase vector of $(\widetilde{\mathbf{x}}(n))_{n\in\mathbb{Z}}$ is defined similarly as $(\mathbf{x}(n))_{n\in\mathbb{Z}}$ and the polyphase transfer matrix of the synthesis FB:

$$\widetilde{\boldsymbol{H}}(\ell) = \left(\widetilde{h}_j(N\ell-i)\right)_{0\leq i<N, 0\leq j<M}, \quad \ell \in \mathbb{Z}. \tag{3}$$

These expressions hold for any oversampled FB.

2.2. Perfect reconstruction

Perfect reconstruction (PR) is an important property in transform processing. One advantage of the polyphase formulation is that PR can be shown[20] to be equivalent to the existence of a matrix $\widetilde{\boldsymbol{H}}[z]$ in $\mathbb{C}[z, z^{-1}]^{N\times M}$ such that:

$$\widetilde{\boldsymbol{H}}[z]\,\boldsymbol{H}[z] = \boldsymbol{I}_N.$$

In a previous work,[21] we have proposed a method to check whether a given oversampled FIR analysis FB can be inverted by an FIR synthesis FB. We suppose in the remaining of this article that the polyphase matrix $\boldsymbol{H}[z]$ is proven to be left invertible. In this case, there exists an integer p such that the polyphase transfer function of the synthesis FB reads: $\widetilde{\boldsymbol{H}}[z] = \sum_{\ell=1-p}^{0} \widetilde{\boldsymbol{H}}(\ell) z^{-\ell}$.

We obviously have

$$\widetilde{\boldsymbol{H}}[z]\boldsymbol{H}[z] = \sum_{\ell=1-p}^{0} \widetilde{\boldsymbol{H}}(\ell) z^{-\ell} \sum_{\ell=0}^{k-1} \boldsymbol{H}(\ell) z^{-\ell} = \sum_{\ell=1-p}^{k-1} \boldsymbol{U}(\ell) z^{-\ell},$$

where

$$\boldsymbol{U}(\ell) = \sum_{s=1+\max(\ell-k,-p)}^{\min(0,\ell)} \widetilde{\boldsymbol{H}}(s)\boldsymbol{H}(\ell-s). \tag{4}$$

The PR property is then equivalent to $\boldsymbol{U}(\ell) = \delta_\ell \boldsymbol{I}_N$, which leads to the following linear equation:

$$\mathcal{H}\widetilde{\mathcal{H}} = \mathcal{U}, \tag{5}$$

where

$$\begin{aligned} \widetilde{\mathcal{H}}^\top &= \left[\widetilde{\boldsymbol{H}}(1-p), \cdots, \widetilde{\boldsymbol{H}}(0)\right], \\ \mathcal{U}^\top &= \left[\boldsymbol{0}_{N,(p-1)N}\ \boldsymbol{I}_N\ \boldsymbol{0}_{N,(k-1)N}\right], \end{aligned}$$

and

$$\mathcal{H}^\top = \begin{pmatrix} \boldsymbol{H}(0) & \cdots & \boldsymbol{H}(k-1) & & 0 \\ & \ddots & & \ddots & \\ 0 & & \boldsymbol{H}(0) & \cdots & \boldsymbol{H}(k-1) \end{pmatrix}.$$

We have to solve the above system for increasing values of p in order to find the minimum order for an inverse polyphase transfer matrix.

2.3. Optimized FB

The considered FBs are oversampled. Thus, the inverse transform, when one exists, is not unique. In a previous work,[22] we proposed a method to exploit the freedom degrees to select synthesis FB with good frequency selection properties. More precisely, we propose to minimize the following cost function on the impulse responses $(\widetilde{h}_j)_{0\le j<M}$, where for all $0 \le j < M$, $f_j \in [-1/2, 1/2[$ is the frequency around which the frequency response of the filter $\widetilde{H}_j$ should be concentrated:

$$J(\widetilde{H}) = \sum_{j=0}^{M-1} \frac{\int_{-1/2+f_j}^{1/2+f_j} (\nu - f_j)^2 \left|\widetilde{h}_j[\nu]\right|^2 d\nu}{\int_{-1/2+f_j}^{1/2+f_j} \left|\widetilde{h}_j[\nu]\right|^2 d\nu}, \tag{6}$$

where $\widetilde{h}_j[.]$ is the frequency response defined by:

$$\forall \nu \in [-1/2, 1/2[, \quad \widetilde{h}_j[\nu] = \sum_{\ell=1-p}^{0} \sum_{i=0}^{N-1} \widetilde{H}_{i,j}(\ell) e^{-2\imath\pi(N\ell-i)\nu}.$$

The optimization is performed under the constraint on $(\widetilde{h}_j)_{0\le j<M}$ given by (5).

This constrained optimization problem can be rewritten as an unconstrained form, more suitable to further optimization. A singular value decomposition is performed on the matrix $\mathcal{H}$, leading to:

$$\mathcal{H} = \mathcal{U}_0 \Sigma_0 \mathcal{V}_0^*,$$

where $\Sigma_0 \in \mathbb{C}^{r\times r}$ is an invertible diagonal matrix, $\mathcal{U}_0 \in \mathbb{C}^{N(k+p-1)\times r}$ and $\mathcal{V}_0 \in \mathbb{C}^{Mp\times r}$ are semi-unitary matrices and with r the rank of $\mathcal{H}$. Hence, there exist matrices $\mathcal{V}_1 \in \mathbb{C}^{Mp\times(Mp-r)}$ and $\mathcal{U}_1 \in \mathbb{C}^{N(k+p-1)\times(N(k+p-1)-r)}$ such that $[\mathcal{U}_0\, \mathcal{U}_1]$ et $[\mathcal{V}_0\, \mathcal{V}_1]$ are unitary.

Let us call $\widetilde{\mathcal{H}}^0$ a solution of (5). For instance $\widetilde{\mathcal{H}}^0 = \mathcal{H}^\sharp \mathcal{U}$, where $\mathcal{H}^\sharp = \mathcal{V}_0\Sigma_0^{-1}\mathcal{U}_0^*$ is the pseudo-inverse of $\mathcal{H}$. Equation (5) becomes:

$$\mathcal{U}_0\Sigma_0\mathcal{V}_0^*(\widetilde{\mathcal{H}} - \widetilde{\mathcal{H}}^0) = \boldsymbol{0}_{(N+k-1)\times N}.$$

It follows that:

$$\mathcal{V}_0^*(\widetilde{\mathcal{H}} - \widetilde{\mathcal{H}}^0) = \boldsymbol{0}_{r\times N},$$

and using the fact that $\mathrm{Ker}(\mathcal{V}_0^*) = \mathrm{Vect}(\mathcal{V}_1)$ we deduce:

$$\widetilde{\mathcal{H}} = \mathcal{V}_1\mathcal{C} + \widetilde{\mathcal{H}}^0, \tag{7}$$

where $\mathcal{C}$ is a matrix of $\mathbb{C}^{(Mp-r)\times N}$.

For all $\ell \in \{1-p, \dots, 0\}$, $j \in \{0, \dots, M-1\}$ and $n \in \{0, \dots, Mp-r-1\}$, we define the matrices:

$$\boldsymbol{V}_j(\ell, n) = \mathcal{V}_1\big((\ell+p-1)M + j, n\big),$$

with $\mathcal{V}_1 = [\mathcal{V}_1(q,n)]_{0\le q<Mp, 0\le n<Mp-r}$. Using (7), it follows that:

$$\widetilde{H}_{i,j}(\ell) = \sum_{n=0}^{Mp-r-1} \boldsymbol{V}_j(\ell,n)\mathcal{C}(n,i) + \widetilde{H}^0_{i,j}(\ell), \tag{8}$$

with $\mathcal{C} = [\mathcal{C}(n,i)]_{0\le n<Mp-r, 0\le i<N}$. We then define the kernel:

$$\begin{aligned} K_j(i,\ell) &= \int_{-1/2+f_j}^{1/2+f_j} (\nu - f_j)^2 e^{-2\imath\pi(N\ell - i)\nu} d\nu \\ &= \begin{cases} \frac{1}{12} & \text{if } i = \ell = 0 \\ \dfrac{(-1)^{N\ell-i} e^{-2\imath\pi(N\ell-i)f_j}}{2\pi^2(N\ell-i)^2} & \text{else} \end{cases} \end{aligned}$$

where $(i,\ell) \in \{1-N, ..., N-1\} \times \{1-p, ..., p-1\}$, and the norm:

$$\|A\|^2_{K_j} = \sum_{(i,i',\ell,\ell')} A_{i,\ell}\overline{A_{i',\ell'}} K_j(i-i', \ell-\ell'),$$

with $(i,i',\ell,\ell') \in \{0,...,N-1\}^2 \times \{1-p,...,0\}^2$. Equation (8) becomes:

$$\int_{-1/2+f_j}^{1/2+f_j} (\nu - f_j)^2 \left|\widetilde{h}_j[\nu]\right|^2 d\nu = \left\| \boldsymbol{V}_j\mathcal{C} + \boldsymbol{H}^0_j \right\|^2_{K_j}.$$

Finally, we introduce the kernel: $\Lambda = (\delta_i\delta_\ell)_{(i,\ell)\in\{1-N,...,N-1\}\times\{1-p,...,p-1\}}$, and thanks to Parseval's theorem, we obtain:

$$\int_{-1/2+f_j}^{1/2+f_j} \left|\widetilde{h}_j[\nu]\right|^2 d\nu = \sum_{\ell=1-p}^{0}\sum_{i=0}^{N-1} \left|\widetilde{H}_{i,j}(\ell)\right|^2 = \left\| \boldsymbol{V}_j\mathcal{C} + \boldsymbol{H}^0_j \right\|^2_{\Lambda}.$$

Thus, by substituting the latter expressions in (6), the constrained optimization problem of J is rewritten as an unconstrained one on $\widetilde{J}$ since:

$$J(\widetilde{h}) = \sum_{j=0}^{M-1} \frac{\left\| \boldsymbol{V}_j\mathcal{C} + \boldsymbol{H}^0_j \right\|^2_{K_j}}{\left\| \boldsymbol{V}_j\mathcal{C} + \boldsymbol{H}^0_j \right\|^2_{\Lambda}} = \widetilde{J}(\mathcal{C}).$$

2.4. Hermitian symmetry

It is well known that the Fourier transform of a real signal leads to a frequency decomposition symmetric for the real parts and anti-symmetric for the imaginary parts, also called Hermitian symmetry. Conversely, if a spectrum exhibits Hermitian symmetry in the frequency domain, the reconstructed signal is real.

This property is mandatory for real data filtering applications, which often consists in removing coefficients in the frequency domain following by their reconstruction. Thus, given that inverse FBs do not always preserve Hermitian symmetry, it is desirable to ensure a reconstruction in the real domain.

In other words, to enforce this property in the synthesis filters, we have to verify that any signal $(y_i(n))_{0\leq i<M}$, such that $y_i(n) = 0$ except for given $j_f \in \{0, ..., M-1\}$ and $n_f \in \mathbb{Z}$ where $y_{j_f}(n_f) = \overline{y_{M-1-j_f}(n_f)}$, is reconstructed as a real signal.

The reconstructed signal reads:

$$\widetilde{x}(m) = \sum_{j=0}^{M-1} \sum_{\ell=-\infty}^{\infty} \widetilde{h}_j(m-N\ell)y_j(\ell) = \widetilde{h}_{j_f}(m-n_fN)y_{j_f}(n_f) + \widetilde{h}_{M-1-j_f}(m-n_fN)y_{j_f}(n_f).$$

A sufficient condition for $\widetilde{x}(m) \in \mathbb{R}$ is $\widetilde{h}_{j_f}(m-n_fN) = \overline{\widetilde{h}_{M-1-j_f}(m-n_fN)}$. This condition must be verified for any (j_f, n_f) couple. Then the sufficient condition on the synthesis filters is:

$$\widetilde{h}_j(n) = \overline{\widetilde{h}_{M-1-j}(n)},\ \forall j \in \{0, ..., M-1\} \text{ et } \forall n \in \mathbb{Z}.$$

Using (3) we can rewrite the condition:

$$\widetilde{\boldsymbol{H}}(\ell) = \overline{\widetilde{\boldsymbol{H}}(\ell)}\boldsymbol{J}_M,\ \forall \ell \in \{p-1, ..., 0\}\,. \tag{9}$$

where $\boldsymbol{J}_M$ is:

$$\boldsymbol{J}_M = \begin{pmatrix} 0 & & 1 \\ & \iddots & \\ 1 & & 0 \end{pmatrix}.$$

Let us assume that the analysis FB is such that:

$$\boldsymbol{H}(\ell) = \boldsymbol{J}_M\overline{\boldsymbol{H}(\ell)}. \tag{10}$$

Using this formulation in (4), we get:

$$\begin{aligned}\boldsymbol{U}(\ell) &= \sum_{s=1+\max(\ell-k,-p)}^{\min(0,\ell)} \widetilde{\boldsymbol{H}}(s)\boldsymbol{H}(\ell-s) \\ &= \sum_{s=1+\max(\ell-k,-p)}^{\min(0,\ell)} \widetilde{\boldsymbol{H}}(s)\boldsymbol{J}_M\overline{\boldsymbol{H}(\ell-s)} \\ &= \sum_{s=1+\max(\ell-k,-p)}^{\min(0,\ell)} \overline{\widetilde{\boldsymbol{H}}(s)}\boldsymbol{J}_M\boldsymbol{H}(\ell-s)\,,\end{aligned}$$

with the hypothesis that the matrix $\boldsymbol{U}(\ell)$ is real and consequently invariant by complex conjugation.

We deduce that if $\widetilde{\mathcal{H}}^\top = \left[\widetilde{\boldsymbol{H}}(1-p), \cdots, \widetilde{\boldsymbol{H}}(0)\right]$ satisfies the linear system (5) then, under the Hermitian symmetry hypothesis on the analysis FB, $\widetilde{\mathcal{H}_2}^\top = \left[\overline{\widetilde{\boldsymbol{H}}(1-p)}\boldsymbol{J}_M, \cdots, \overline{\widetilde{\boldsymbol{H}}(0)}\boldsymbol{J}_M\right]$ is also a solution. Finally, it follows that the sum: $\widetilde{\mathcal{H}_0}^\top = \frac{1}{2}(\widetilde{\mathcal{H}}^\top + \widetilde{\mathcal{H}_2}^\top)$ is a solution too. By construction, this matrix satisfies (9).

3. APPLICATION AND RESULTS

In this section, we first evaluate the improvement in frequency selection of the inverse FB gained from optimization. We finally compare reconstruction quality with FB and STFT methods on simulated as well as real data.

3.1. Optimized and symmetric Filter Banks

We use the following complex analysis FB:

$$h_i(n) = \sin\left(\frac{n\pi}{kN+1}\right)\frac{1}{\sqrt{k'N}}e^{-\imath(i-\frac{k'N}{2}+\frac{1}{2})(n-\frac{kN}{2}-\frac{1}{2})\frac{2\pi}{k'N}},$$

for all $1 \leq n \leq kN$ and $0 \leq i \leq k'N-1$. It is interesting to note that this FB offers the Hermitian property (10). For this first application we have worked with the following parameters: $N = 16$, $k = 3$ and $k' = 7/4$.

The method of Section 2.2 is applied to compute a synthesis FB (thus leading to a polyphase inverse matrix of order $p = 3$). This FB is then converted into a symmetric one using the method described in Section 2.4, followed by optimization. On Figure 2, the frequency responses of the different filter banks are shown. As expected, the frequency responses of the analysis filter bank display are well behaved, unlike its pseudo-inverse or symmetric versions, while the proposed optimized filter bank shows a far better frequency selection.

3.2. Spectral Analysis

3.2.1. Simulated data

Using the previously constructed symmetric and optimized filter bank, we now apply them to time-frequency representation and selection. In this application, the filter length is 48 and the number of considered frequencies is 28. We chose the STFT parameters to match the number of frequencies and the sample shift ($N = 16$ samples) of the chosen FB.

A first test is performed on simulated data: a sinusoidal signal is corrupted by a white Gaussian noise and another sine function, thus adding an unwanted frequency in the signal. In the frequency domain, corresponding coefficients were kept in the STFT and FB methods and used for reconstruction. As can be seen in Table 1, for noisy data with an SNR of 4.45dB the STFT achieves 7.9dB while with an optimized filter bank it is possible to reconstruct a signal with an SNR of 14.4dB. It is also interesting to note that the optimization process helped in improving the reconstruction results, with a gain of about 2dB when using the optimized version. On Figure 3 we compare see the original and noisy signals as well as the different reconstructions.

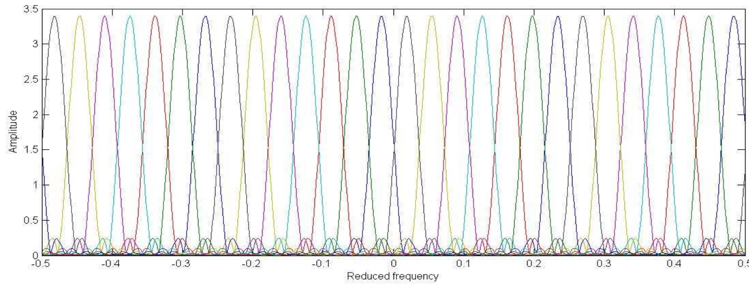

(a)

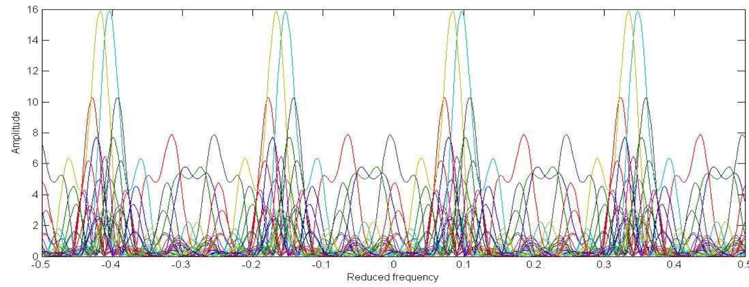

(b)

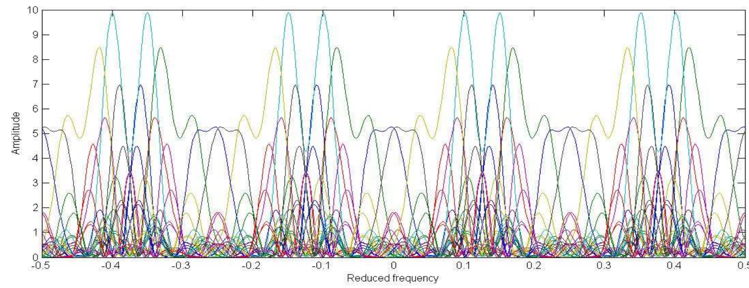

(c)

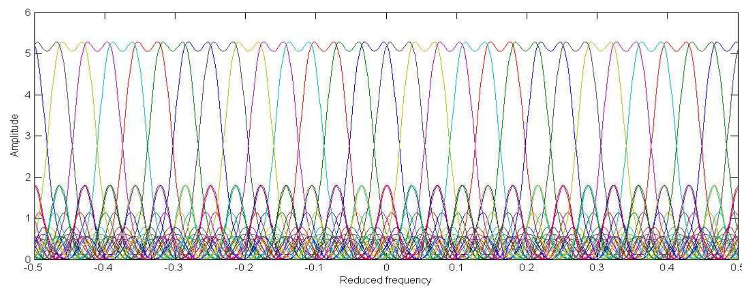

(d)

Figure 2. Frequency response of (a) the analysis FB, (b) the pseudo-inverse synthesis FB, (c) the Hermitian symmetric FB and of (d) the optimized FB.

	Noisy data	STFT	Symmetric FB	Optimized FB
SNR	4.45dB	7.9dB	12.2dB	14.4dB

Table 1. Signal to Noise ratio in dB after reconstruction with different methods.

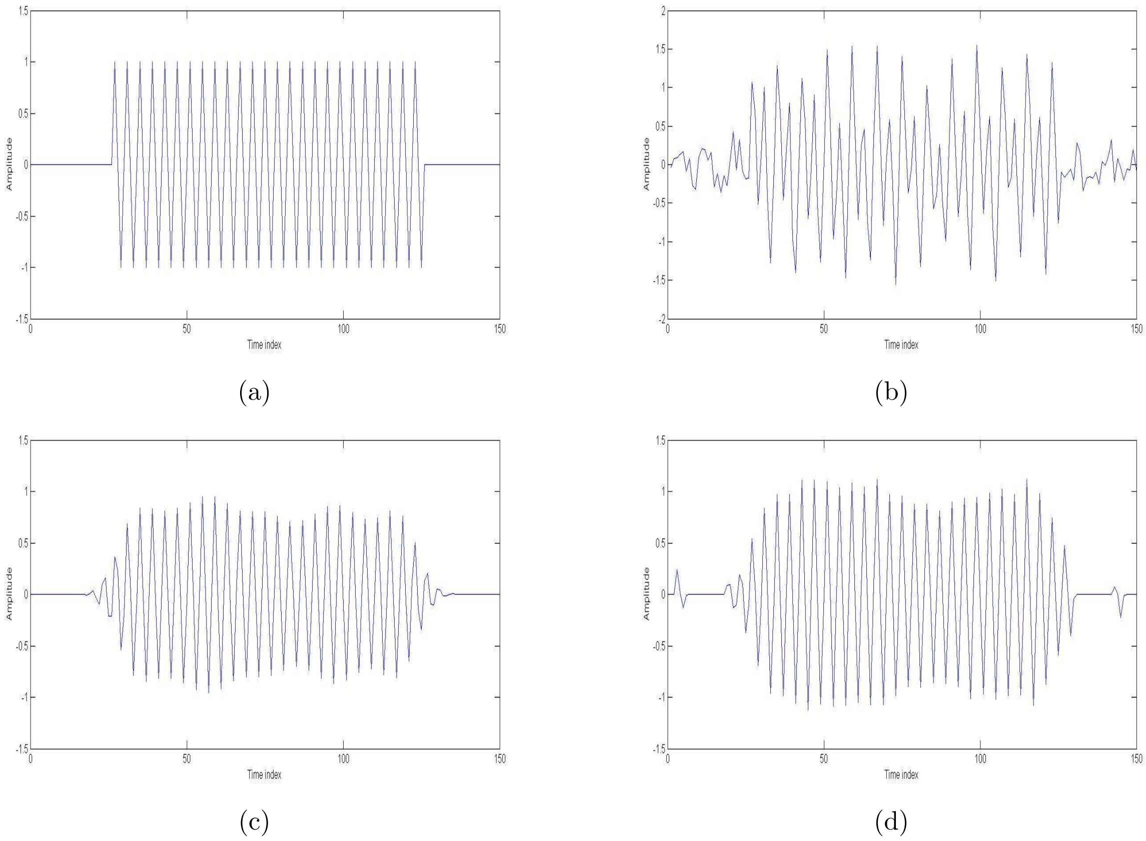

Figure 3. (a) Original signal, (b) noisy signal, (c) reconstructed signal using STFT, (d) reconstructed signal using an optimized synthesis FB.

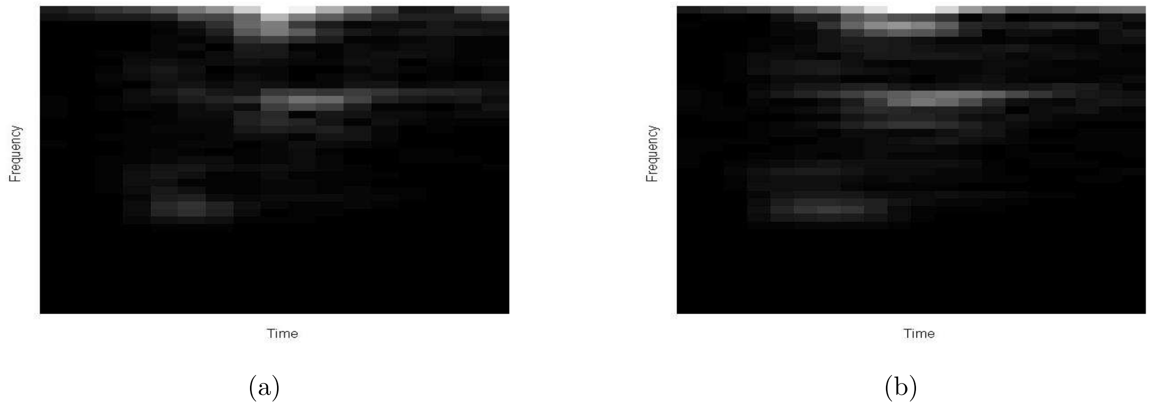

Figure 4. Time-frequency representation using (a) the STFT and (b) FB transform.

3.2.2. Real data

The second experimentation is carried on a vibration signal from a car engine. Information extracted from the in-cylinder pressure signal are important for combustion control. Unfortunately in-cylinder sensors are expensive and have a short life expectancy, hence an alternative must be found for mass production. Pressure gradients in the cylinder chamber produce vibrations propagating through the engine structure. It is therefore interesting to obtain information on the in-cylinder gradient pressure by working on vibration signals only. Those vibrations are recorded by cheaper knock sensors but are corrupted by multiple noises and unwanted frequencies corresponding to other engine events (*e.g.* injection).

For this application, we have considered the knock signal displayed on Figure 5(b). We have chosen an analysis FB with parameters $N = 16$, $k = 7$ and $k' = 5$ thus leading to 80 frequency components. The time-frequency representation of this signal can be seen on Figure 4 using both the STFT and FB transforms. The strategy used here consists in keeping only the coefficients with high magnitude (in white) in the lower frequency bands, as well as their immediate neighbors. The goal is to isolate the combustion related part, represented by a peak in the pressure gradient signal (Figure 5(a)). Reconstruction results show that both methods succeed in isolating the pressure gradient peak, thus validating the proposed strategy. We can also see that the shape of the peak when using the optimized FB reconstruction is closer to the pressure gradient peak than when using the inverse STFT.

4. CONCLUSION

In this article we have shown how to construct and optimize filter banks in the oversampled and overlapping case. We have also proposed a method to build Hermitian symmetric filter banks (under the assumption that the analysis FB shares the same property). Those FBs were then used to perform spectral analysis and were compared to the classical STFT, improving reconstruction properties in localized T-F filtering on simulated as well as real data.

REFERENCES

1. P. Flandrin, *Time-frequency and time-scale analysis*, Academic Press, San Diego, USA, 1998.

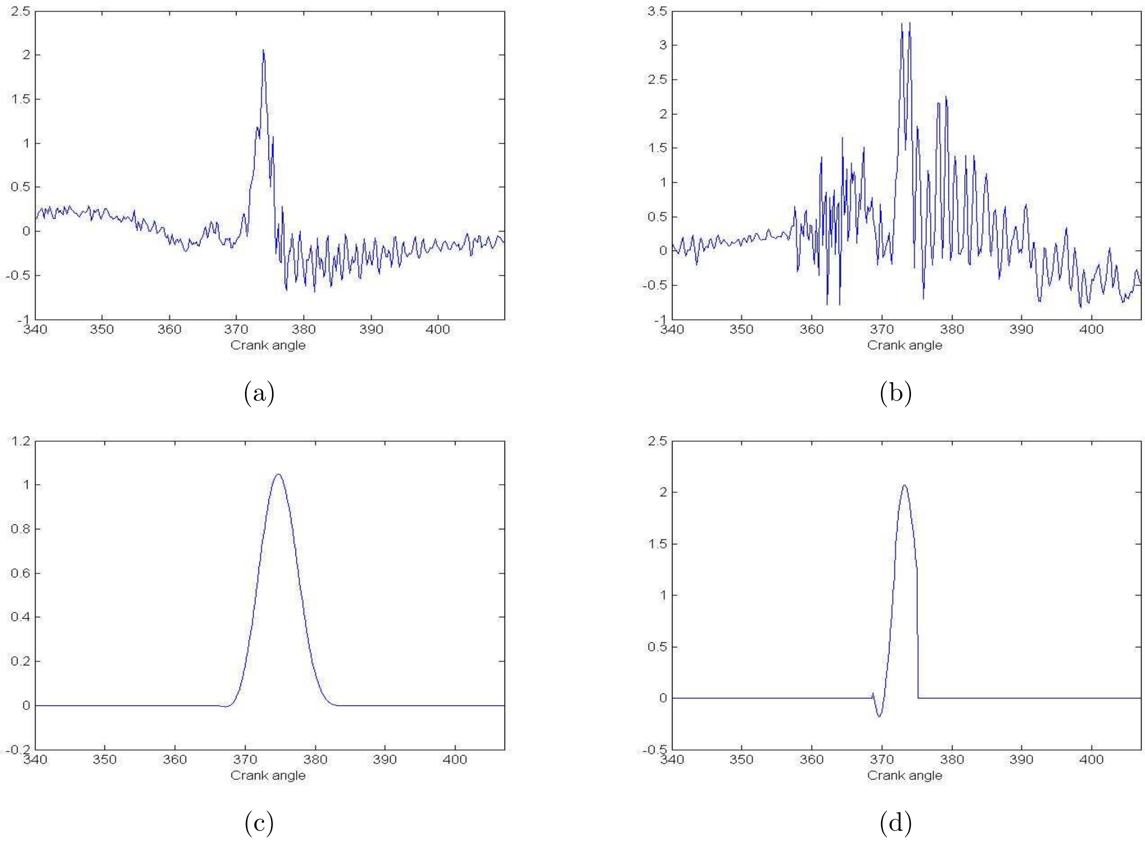

Figure 5. (a) Pressure gradient signal, (b) knock signal, (c) reconstructed signal using STFT, (d) reconstructed signal using an optimized synthesis FB.

2. I. Daubechies, *Ten Lectures on Wavelets*, CBMS-NSF, SIAM Lecture Series, Philadelphia, PA, USA, 1992.
3. A. H. Nuttall, "Some windows with very good sidelobe behavior," *IEEE Trans. on Acous., Speech and Signal Proc.* **29**, pp. 84–91, Feb. 1981.
4. J. Allen, "Short-term spectral analysis, synthesis, and modification by discrete Fourier transform," *IEEE Trans. on Acous., Speech and Signal Proc.* **25**, pp. 235–238, Jun. 1977.
5. R. E. Crochiere, "A weighted overlap-add method of short-time Fourier analysis/synthesis," *IEEE Trans. on Acous., Speech and Signal Proc.* **28**, pp. 99–102, Feb. 1980.
6. M. Kramer and D. Jones, "Improved time-frequency filtering using an STFT analysis-modification-synthesis method," in *Proc. of the IEEE-SP International Symposium on Time-Frequency and Time-Scale Analysis*, pp. 264–267, (Philadelphia, PA, USA), Oct. 25-28 1994.
7. M. R. Portnoff, "Time scale modification of speech based on short-time Fourier analysis," *IEEE Trans. on Acous., Speech and Signal Proc.* **29**, pp. 374–390, Apr. 1981.
8. K. Gröchenig, "Irregular sampling of wavelet and short-time Fourier transform," *Constr. Approx.* **9**(2-3), pp. 283–297, 1993.
9. H.-G. Feichtinger, W. Kozek, and T. Strohmer, "Reconstruction of signals from irregular samples of its short-time Fourier transform," in *Proc. SPIE, Wavelets Applications in Signal and Image Processing*, A. F.

Laine, M. A. Unser, and M. V. Wickerhauser, eds., **2569**, pp. 140–150, (San Diego, CA, USA), July 9-14 1995.

10. Z. Cvetković and M. Vetterli, “Overampled filter banks,” *IEEE Trans. on Signal Proc.* **46**, pp. 1245–1255, May 1998.
11. H. Bölcskei, F. Hlawatsch, and H. G. Feichtinger, “Frame-theoretic analysis of oversampled filter banks,” *IEEE Trans. on Signal Proc.* **46**, pp. 3256–3268, Dec. 1998.
12. J. Zhou and M. N. Do, “Multidimensional oversampled filter banks,” in *Proc. SPIE, Wavelets Applications in Signal and Image Processing*, M. Papadakis, A. F. Laine, and M. A. Unser, eds., **5914**, pp. 591424.1–591424.12, (San Diego, CA, USA), Jul. 31 - Aug. 3 2005.
13. A. Chebira and J. Kovačević, “Lapped tight frame transforms,” in *Proc. Int. Conf. on Acoust., Speech and Sig. Proc.*, **3**, pp. 857–860, (Honolulu, HI, USA), Apr. 15-20 2007.
14. R. Bernardini, M. Durigon, R. Rinaldo, A. Vitali, , and P. Zontone, “Frame-based multiple-description video coding with extended orthogonal filter banks,” *EURASIP J. Appl. Sign. Proc.* **2006**, p. 17, 2006.
15. L.-T. Nguyen, A. Belouchrani, K. Abed-Meraim, and B. Boashash, “Separating more sources than sensors using time-frequency distributions,” *EURASIP J. Appl. Sign. Proc.* **2005**(17), pp. 2828–2847, 2005.
16. K. S. C. Pun and T. Q. Nguyen, “Design of oversampled filter bank based widely linear OQPSK equalizer,” in *Proc. Int. Conf. on Acoust., Speech and Sig. Proc.*, **3**, pp. 861–864, (Honolulu, HI, USA), Apr. 15-20 2007.
17. J. Gauthier, M.-C. Cacas, and L. Duval, “Local directional and uncoherent seismic noise filtering with oversampled filter banks,” in *Workshop of the EAGE Conference and Technical Exhibition*, (London, UK), Jun. 11-14 2007.
18. J. Gauthier, L. Duval, and J. C. Pesquet, “Inversion and optimization of oversampled complex filter banks: applications to directional filtering of images,” *IEEE Trans. on Signal Proc.* , 2007. Submitted.
19. H. S. Malvar, *Signal processing with Lapped Transforms*, Artech House, Norward, MA, USA, 1992.
20. P. P. Vaidyanathan, *Multirate systems and filter banks*, Prentice Hall, 1993.
21. J. Gauthier, L. Duval, and J. C. Pesquet, “Low redundancy oversampled lapped transforms and application to 3D seismic data filtering,” in *Proc. Int. Conf. on Acoust., Speech and Sig. Proc.*, **2**, pp. 821–824, (Toulouse, France), May 14-19 2006.
22. J. Gauthier, L. Duval, and J. C. Pesquet, “Oversampled inverse complex lapped transform optimization,” in *Proc. Int. Conf. on Acoust., Speech and Sig. Proc.*, **1**, pp. 549–552, (Honolulu, HI, USA), Apr. 15-20 2007.